

MEASUREMENTS OF THE SPECTRAL PROFILE OF BALMER ALPHA  
EMISSION FROM THE HYDROGEN GEOCORONAJ. W. Meriwether, Jr., S. K. Atreya and T. M. Donahue  
Space Physics Research Laboratory, Department of Atmospheric  
and Oceanic Science, The University of Michigan, Ann Arbor, Michigan 48109R. G. Burnside  
Department of Physics, University of Puerto Rico  
Rio Piedras, Puerto Rico 00931

*Abstract.* Instrumental improvements responsible for a factor of 25 increase in the sensitivity of the Fabry-Perot interferometer enable us to observe for the first time the short wavelength depletion of the Balmer  $\alpha$  spectral profile due to hydrogen escape. These results are shown to be consistent with the implications of OGO-5 observations by Bertaux.

## INTRODUCTION

Because the geocorona is optically thin at the wavelength of the atomic hydrogen Balmer alpha ( $H\alpha$ ) emission line at 6562.8Å, ground-based observations at high spectral resolution of the spectral profile of  $H\alpha$ , produced by hydrogen fluorescence of Lyman  $\beta$  photons, are linked directly to measurements of the velocity distribution of hydrogen atoms. Chamberlain [1976] and Prisco and Chamberlain [1978; 1979] have made extensive calculations concerning the expected shape for the zenith orientation, but the predicted departures from the Maxwellian profile are small and difficult to observe. The first observations of the  $H\alpha$  spectral profile at high resolution were made by Atreya et al. [1975] with a Fabry-Perot interferometer of low sensitivity (0.05 counts/secR). By averaging all observations obtained each night, values for the apparent thermal width were found to lie in the range between 700 and 850K.

Major improvements over the years increasing the sensitivity of the Fabry-Perot by a factor of 25 encouraged us to undertake new observations. We chose to use the Fabry-Perot interferometer at the Arecibo Observatory because simultaneous measurements of the oxygen ion temperature with the incoherent scatter radar would be possible. At night the assumption can be made that the ion temperature will be equal to the neutral thermospheric temperature. For levels of high magnetic activity, theory [Atreya, 1973; Fahr, 1976] suggests the hydrogen atoms in the transition region below the exobase will be cooled by the escaping component, and a temperature difference between hydrogen and oxygen atoms will develop. Joint optical and radar observations were carried out at Arecibo in March, 1980, with Vincent Wickwar and Suman Ganguly to seek this effect, but the magnetic activity was very quiet. Instead, we found that we were able to detect the cooling that results from the escape of hydrogen atoms. We present these optical observations in this paper.

## INSTRUMENTATION

The improvement of the sensitivity of the Fabry-Perot interferometer relative to the early work of Atreya et al. [1975] was achieved by replacing or modifying four components of the instrument, i.e., photomultiplier, interference filter, aperture diameter, and the pressure scanning system. The use of a RCA 31034A-02 red-sensitive photomultiplier with a dark count less than 1 c/s when cooled to  $-50$  C increased the sensitivity by 400%. Isolation of  $H\alpha$  was achieved with a three cavity interference filter, 6.2Å in spectral width and 55% peak transmission. The higher transmission of this filter increased the throughput by 60%. The rejection in the wings of the transmission passband of this filter blocked the OH contamination from the P branch rotational lines of the (6-1) band at 6569.0Å ( $H\alpha + 6.2\text{Å}$ ) and 6553.7Å ( $H\alpha - 9.1\text{Å}$ ); this was con-

firmed by transmission calibration of the filter [Meriwether, 1975]. The better wing rejection led to the increase of the aperture size by a factor of two over that used by Atreya [1973]. In the earlier work maximum spectral resolution was needed to isolate the OH contamination. The doubling of the aperture diameter increased the sensitivity by 400%.

In the work by Atreya et al. [1975], galactic contamination was a serious problem because of the long integration times required. The extent of the unwanted radiation was reduced by the use of a small field of view and by tracking a region of the sky free of galactic emission. The higher ratio of signal to noise of our observations allowed us to relax these restrictions. We found it easy to identify galactic contamination in a seven minute scan as the fringe would be grossly distorted by the great width and Doppler shift of the galactic  $H\alpha$  fringe. The affected scans were removed and the remainder of the data averaged over 0.75 hours for each data set.

The reflectivity of the etalon plate coatings for the Arecibo interferometer is 92% at 6563Å, higher than the value of 83% applicable for the instrument used by Atreya et al. [1975]. This improves the spectral resolution but our total gain in sensitivity is reduced a factor of two.

Calibration of the instrumental profile with a He-Ne frequency stabilized laser indicated a total finesse of 13.4; the aperture broadening was minor. The wavelength scanning system consists of a piston attached to a stepping motor and designed to move upon pulse command in a smooth cylinder, which is linked by tubing to the etalon chamber. This system may be programmed to scan a selected wavelength range in the region where the  $H\alpha$  emission appears [Meriwether, 1979]. The increase in sampling time afforded by this mode of scanning as compared with Atreya et al. [1975] gave a factor of 2 enhancement in signal. The net gain in sensitivity was a factor of 25 due to above mentioned factors about photomultiplier tube, filter, aperture, etalon reflectivity and sampling time.

The etalon spacer thickness used for our observations was 0.25 cm, identical to that used by Atreya et al. [1975], and corresponds to a free spectral range of 0.86Å at 6563Å or 39.3 km/sec of total Doppler shift. Location of the geocoronal hydrogen line in the spectral scan was determined by examination of the spectral profile of a hydrogen lamp [Atreya et al., 1975].

Absolute intensity calibration of the interferometer was obtained by cross calibration against simultaneous observations of  $H\alpha$  with a 1 m spectrophotometer [Meriwether, 1979; Meriwether and Walker, 1980; Burnside et al., 1980]. We estimate the accuracy of our results to be better than  $\pm 35\%$ .

## OBSERVATIONS

We used two illumination geometries in these observations, zenith and horizon. In the first, we made measurements over a span of 15 minutes in the zenith with wavelength scans covering 35 channels. In the second, the measurements were made in the vicinity of the North Star at a zenith angle of 60 degrees. In both cases galactic contamination was not serious. Moreover, an unsuccessful search was made for the large galactic Doppler shift that should be present for a galactic source. The observed Doppler shift was less than 200m/s to the east in agreement with the magni-

tude of typical thermospheric winds. In all observations the sky was very clear and the moon was below the horizon.

Magnetic activity was very quiet on 14/15 March, 1980, with a  $\Sigma Kp$  value of 12 and a pronounced increase in activity from a  $Kp$  of 1 to 3+ midway through the optical observations. The  $F_{10.7}$  cm flux for both nights was between 140 and 150 ( $10^{-22}$  watts/m<sup>2</sup> Hz).

In Figure 1 we show two zenith spectral profiles obtained on 14/15 March, 1980, for times of evening twilight and midnight. For the purpose of comparison of these two fringes, the background continuum measured in the wings of the profile was subtracted, the spectral profile remaining was smoothed with a three point moving average, and these results after normalization to a peak value of 1 are plotted in Figure 2. The midnight profile was shifted to the blue by 0.4 km/sec to correct for instrumental drift.

The alignment of the two fringes on the right signifies a complete ensemble of hydrogen atoms moving away from the observer for either the twilight or midnight fringe. In contrast there is a substantial deficit of hydrogen atoms in the midnight fringe complementing the ensemble of atoms moving downward. That is, the twilight fringe is more symmetrical than the midnight fringe. The implication is easy to see: the missing atoms on the left of the midnight fringe are those that have already escaped and represent outgoing hyperbolic particles. The extension of the velocity deficit to zero reflects the range of escape speeds along the line of sight above the shadow height, since the emitting region is a vertical path through the geocorona terminated at the bottom by the shadow of the Earth and the penumbra generated by multiple scattering into the shadow cone.

The resulting profile when mixed in with the noise attending these measurements appears to be Gaussian with a reduced thermal width. We used an analysis program in which a Gaussian fitting function was convolved with the measured instrumental function to extract 4 parameters-amplitude, peak position, background level, and profile width. Figures 3 and 4 show the results of this analysis. The length of the error bars corresponds to plus or minus two standard deviations. In Figure 2 we also show the variation of the geometrical shadow height over the time span of the measurements for both 12/13 March, 1980, and 14/15 March, 1980. The large variation shown for 14/15 March is important in the interpretation of our results.

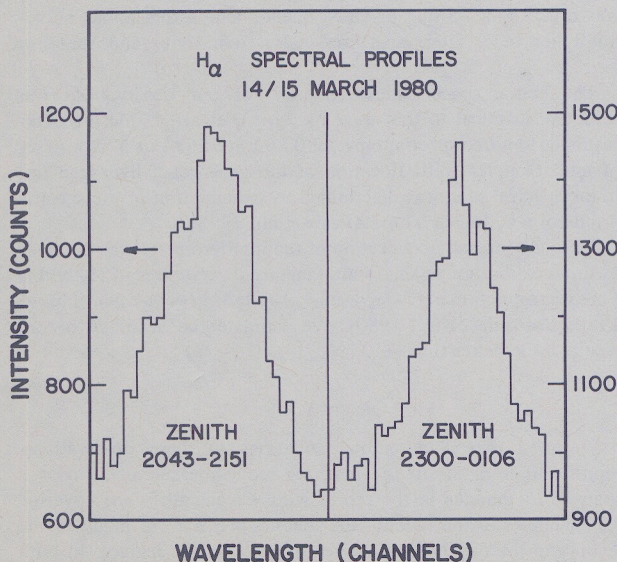


Fig. 1. Zenith measurements of Balmer  $\alpha$  spectral profiles at high resolution for evening twilight and midnight on 14/15 March, 1980. Integration times were 90 and 180 seconds per channel, respectively.

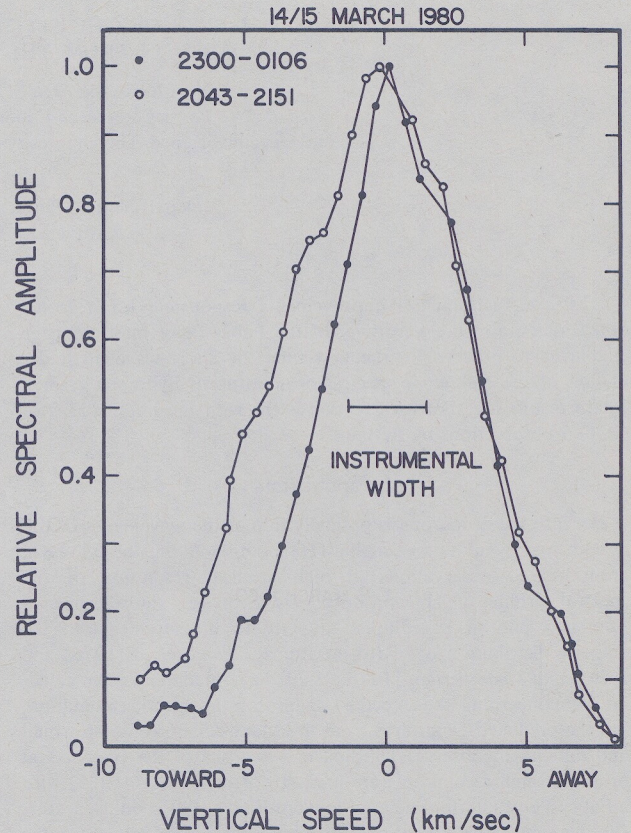


Fig. 2. Comparison of evening twilight and midnight profiles after smoothing and normalization of peak amplitudes.

DISCUSSION

For relatively quiet geomagnetic conditions, the escape of hydrogen from the exobase is governed primarily by a mechanism which involves resonance charge exchange between low energy neutral hydrogen atoms and fast plasmaspheric protons [Tinsley, 1978; Liu and Donahue, 1974a, b, c; Cole, 1966]. With increasing exobase temperature, the proportion of atoms escaping due to their large thermal velocity rises. At exobase temperatures above 1200K, the Jeans mechanism of thermal escape dominates over charge exchange. According to Hunten and Donahue [1976] the Jeans escape flux is on the order of 10% of the charge exchange escape flux for exobase temperature of 900K. This percentage rises to about 65% for a temperature of 1200K, and to about 325% for an exobase temperature of 1900K. The increasing exobase temperature, therefore, results in a depletion of high velocity component of the Doppler spectral profile due to increased escape.

The charge exchange mechanism will also result in a depletion of the  $H\alpha$  profile for incoming particles. The exchange of a cold neutral atom for a hot ion will enhance the fraction of hyperbolic particles present in outgoing orbits. Therefore, the temperature retrieved from the measured spectral profile represents the "effective" temperature of a velocity distribution that is highly anisotropic averaged over a slant path many thousand kilometers long.

Two outstanding features are observed in the results of the thermal width analysis for March 14/15, 1980 (Figure 3): in the early evening twilight the retrieved Doppler temperature is high, between 1200 and 1400K, but towards the middle of the night the retrieved Doppler temperature drops to about 400K. The large decrease in the "effective" temperature observed on March 14/15, 1980, can be explained in part by the drastic change in the illumination geometry for the zenith between evening twilight and midnight. The shadow height changed from 500 km to nearly 20,000 km during this time interval. On the other hand, for the

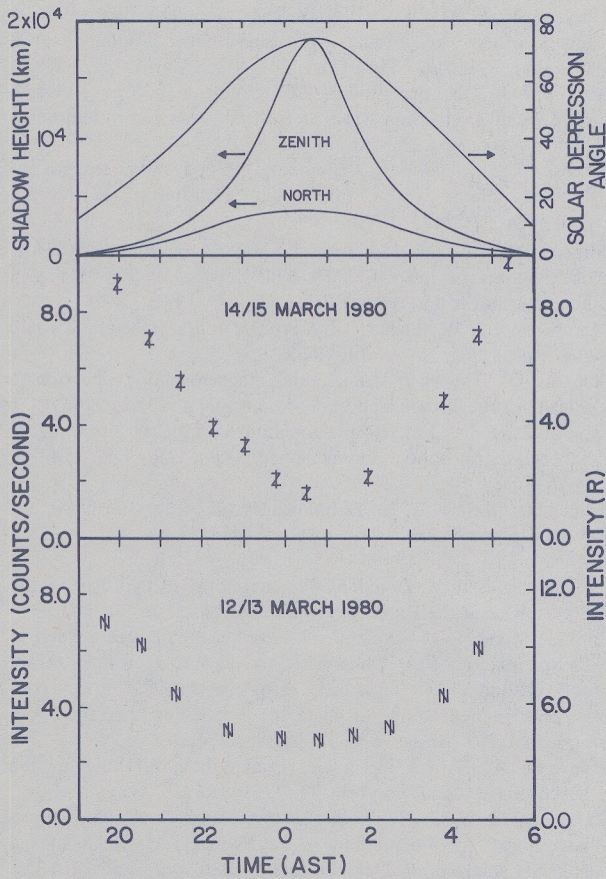


Fig. 3. Composite showing measurements of  $H\alpha$  intensities and shadow heights for northern and zenith instrumental orientations. Intensity error bars span  $\pm 2$  standard deviations.

set of measurements on March 12/13, 1980, where the viewing angle was directed towards the northern horizon, the variation of shadow height from evening to midnight is less severe, i.e., from 500 km to 3,700 km. We note that the escape velocity of hydrogen

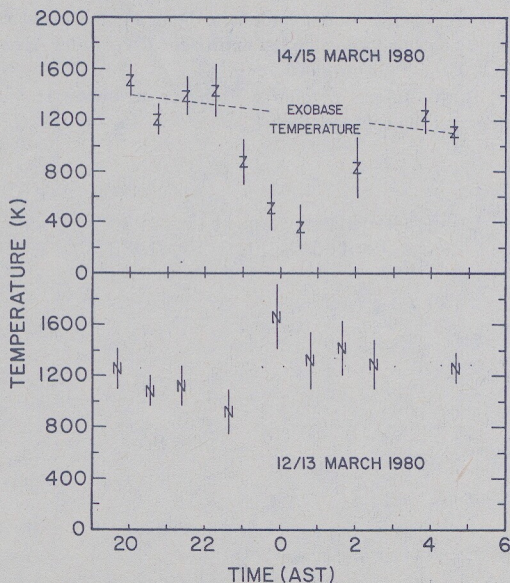


Fig. 4. Temperature plots deduced from apparent thermal width of  $H\alpha$  for 12/13 March and 14/15 March, 1980. Temperature error bars span  $\pm 2$  standard deviations.

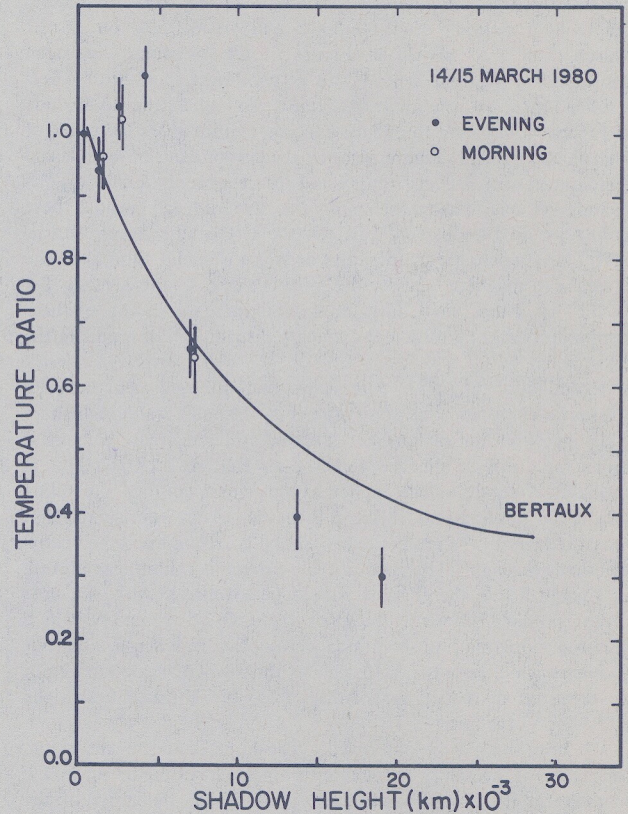


Fig. 5. Comparison of relative temperatures measured on 14/15 March, 1980, with temperature results of Bertaux [1978]. Error bars shown span  $\pm 1$  standard deviation.

atoms is 10.8 km/sec at 500 km, and 5.7 km/sec at 20,000 km; thus, the escape velocity at 20,000 km is comparable to the thermal velocity of hydrogen atoms at 1,200K, which is 4.4 km/s. Therefore, for either the thermal escape or charge exchange mechanism, at high shadow heights a large fraction of the incoming high energy tail of the Doppler profile will be depleted and the remainder of the ensemble of hydrogen atoms will exhibit a smaller velocity dispersion.

Quantitative comparison with theory is difficult because the importance of multiple scattering of Lyman  $\beta$  photons into the shadow cone remains to be assessed. The evaluation of Meier [1969] assumed the exosphere temperature remained constant above the exobase. New calculations by Anderson et al. [1980] have demonstrated the importance of including a model of the non-isothermal spherical distribution of the Lyman  $\beta$  dayglow into the structure of radiative transfer calculations.

The expectation of a large decrease in the thermal width of  $H\alpha$  within the higher region of geocorona at times of high exobase temperatures is supported by results obtained by the hydrogen cell experiment on OGO 5 satellite [Bertaux and Blamont, 1970; Bertaux, 1978]. Mapping of the geocorona indicated a major decrease in the reduction factor (the ratio of the observed Lyman  $\alpha$  intensity with the hydrogen cell absorbing to that observed with the cell switched off) indicating a large decrease in the Lyman  $\alpha$  thermal width as a function of the distance away from the Earth.

We have compared our results to the theoretical calculations of Bertaux [1978] based on the OGO 5 data by normalizing the temperature profile of 14/15 March to the exobase temperature and plotting this set of ratios as a function of shadow height. This procedure, which was applied also to Bertaux's curve, was used to compensate for differences in exobase temperatures between the two sets. Measurements of the thermospheric temperature by the satellite AE-E (courtesy of P. B. Hays and N. W. Spencer) indicate

exobase temperature values of 1350K and 1175K to be reasonable for twilight periods of 1900–2000 and 0400–0500 on 14/15 March, 1980. As shown in Figure 4, our measured hydrogen temperatures for these periods are in good agreement with AE-E results. Linear interpolation between these values, the dotted line in Figure 4, was used to deduce exobase temperatures for times of high shadow height. Figure 5 shows the comparison of normalized temperatures for Bertaux's curve and for the observations of 14/15 March. We do not show the results for 12/13 March because these points would be clustered towards the left of the figure (below 3,700 km) where the temperature decrease is slight. Moreover, the increase in magnetic activity during this night, to the level of 3+ in the Kp index, may have caused an increase in the exobase temperature and perturbed the velocity distribution of atoms in the exosphere.

Examination of Figure 5 indicates that the agreement between Bertaux's curve and our observations is reasonable although there is a suggestion that our measured temperatures decrease somewhat more rapidly with shadow height than Bertaux's curve. This is probably a result of the higher exobase temperatures prevailing during our observations. Also, in this comparison we assumed that measured zenith  $H\alpha$  temperatures can be correlated with geometrical shadow height. This will not be correct if multiple scattering of Lyman  $\beta$  into the shadow should be extensive. Also, we note there is much difference between the OGO-5 geometry which featured horizontal observations across the geocorona and our geometry which is vertical. In view of this, we conclude our zenith observations of the thermal width of  $H\alpha$  are consistent with the OGO-5 observations.

We now summarize our results. The large enhancement in the sensitivity of the Fabry-Perot interferometer has opened up a new method for the groundbased exploration of the dynamics of the hydrogen geocorona. We have shown that the escape of hyperbolic particles has a significant effect on the symmetry of the spectral line profile. Further analysis will require the understanding of the relative roles played by the mechanisms of charge exchange and Jeans escape during solar maximum. A detailed calculation based on Chamberlain's theory of the velocity distribution as a function of height will be necessary for comparison with our observations.

*Acknowledgements.* We acknowledge useful conversations with P. B. Hays, J. C. G. Walker, and B. A. Tinsley. This research was supported by grant number ATM 7901064 and ATM 8009218 from Atmospheric Research section of the National Science Foundation. The Arecibo Observatory is operated by Cornell University under contract from the National Science Foundation.

#### REFERENCES

- Anderson, D. E., Jr., P. D. Feldman, E. P. Gentieu, and R. R. Meier, The UV Dayglow 2,  $Ly\alpha$  and  $Ly\beta$  emissions and the H distributions in the mesosphere and thermosphere, *Geophys. Res. Lett.*, **7**, 529–532, 1980.
- Atreya, S. K., An investigation into the geocoronal and interplanetary hydrogen Balmer emissions. PhD. Thesis, Univ. of Mich., Ann Arbor, 1973.
- Atreya, S. K., P. B. Hays, and A. F. Nagy, Doppler profile measurements of the geocoronal hydrogen Balmer Alpha line, *J. Geophys. Res.*, **80**, 635, 1975.
- Bertaux, J. L., Interpretation of OGO-5 line shape measurements of Lyman- $\alpha$  emission from terrestrial exospheric hydrogen, *Planet. Space Sci.*, **26**, 431, 1978.
- Bertaux, J. L., and J. E. Blamont, OGO-5 measurements of Lyman- $\alpha$  intensity distribution and linewidth up to 6 earth radii, *Space Res.*, **10**, 591, 1970.
- Burnside, R. G., J. W. Meriwether, and J. C. G. Walker, Airglow observations of the OI 7774 multiplet at Arecibo during a magnetic storm, *J. Geophys. Res.*, **85**, 767, 1980.
- Chamberlain, J. W., Spectral line profiles for a planetary corona, *J. Geophys. Res.*, **81**, 1774, 1976.
- Cole, K. D., Theory of some quiet magnetospheric phenomena related to the geomagnetic tail, *Nature*, **211**, 1385, 1966.
- Fahr, H. J., Reduced hydrogen temperatures in the transition region between the thermosphere and exosphere, *Ann. Geophys.*, **25**, 306, 1976.
- Hunten, D. M., and T. M. Donahue, Hydrogen loss from the terrestrial planets. *Ann. Rev. of Earth and Planet. Sci.*, **4**, 265, 1976.
- Liu, S. C., and T. M. Donahue, The aeronomy of hydrogen in the atmosphere of the Earth, *J. Atmos. Sci.*, **31**, 1118, 1974a.
- Liu, S. C., and T. M. Donahue, Mesospheric hydrogen related to exospheric escape mechanisms, *J. Atmos. Sci.*, **31**, 1466, 1974b.
- Liu, S. C., and T. M. Donahue, Realistic model of hydrogen constituents in the lower atmosphere and escape flux from the upper atmosphere, *J. Atmos. Sci.*, **31**, 2238, 1974c.
- Meier, R. R., Balmer alpha and Lyman beta in the hydrogen geocorona, *J. Geophys. Res.*, **74**, 3561, 1969.
- Meriwether, J. W., Jr., High latitude airglow observations of correlated short-term fluctuations in the hydroxyl Meinel 8-3 band intensity and rotational temperature, *Planet. Space Sci.*, **23**, 1211, 1975.
- Meriwether, J. W., Jr., Measurements of weak airglow emissions with a programmable scanning spectrophotometer, *Planet. Space Sci.*, **27**, 1221–1232, 1979.
- Meriwether, J. W., Jr., and J. C. G. Walker, First negative band system of nitrogen in the night sky over Arecibo during geomagnetic storms, *J. Geophys. Res.*, **85**, 1279, 1980.
- Prisco, R. A., and J. W. Chamberlain, Spectral line profiles in a planetary corona; a collisional model, *J. Geophys. Res.*, **83**, 2157, 1978.
- Prisco, R. A., and J. W. Chamberlain, Doppler line profiles in a planetary corona: an extended approach, *J. Geophys. Res.*, **84**, 4363, 1979.
- Tinsley, B. A., Effects of charge exchange involving H and  $H^+$  in the upper atmosphere, *Planet. Space Sci.*, **26**, 847, 1978.

(Received August 5, 1980;  
accepted August 20, 1980.)